PAPER • **OPEN ACCESS**

Ultra-smooth ultrathin silver films deposited on acid treated Silicon substrates

To cite this article: Muhammad Asad *et al* 2020 *Nano Ex.* **1** 020012

NANO EXPRESS

PAPER

Ultra-smooth ultrathin silver films deposited on acid treated Silicon substrates

Muhammad Asad[1,3], **Sohail A Jalil**[1,2], **Mohamed ElKabbash**[2,4] and **Chunlei Guo**[1,2,4]

[1] GPL, Changchun Institute of Optics, Fine Mechanics and Physics, Chinese Academy of Sciences, Changchun 130033, People's Republic of China
[2] The Institute of Optics, University of Rochester, Rochester, NY 14627, United States of America
[3] Present address: Dipartimento di INGEGNERIA, Università degli Studi di Napoli"Parthenope"- Isola C4, Centro Direzionale, 80143 Naples, ITALY
[4] Authors to whom any correspondence should be addressed.

E-mail: melkabba@ur.rochester.edu **and** chunlei.guo@rochester.edu

Keywords: thin films, physical vapor deposition, plasmonic materials

OPEN ACCESS

RECEIVED
26 June 2020

REVISED
7 July 2020

ACCEPTED FOR PUBLICATION
10 July 2020

PUBLISHED
27 July 2020

Abstract

Fabrication of smooth noble metal ultrathin films is crucial to many optical and electronic devices. However, the metals' adatom-adatom cohesive force is usually stronger than the adatom-substrate adhesive force leading to a Vollmer-Weber, island-like, growth mode. This phenomenon imposes limitations on the surface smoothness and minimum (percolation) thickness necessary to obtain a smooth film. Here, we demonstrate a facile method to fabricate ultra-smooth ultrathin silver (Ag) films on silicon via physical vapor deposition. By removing the oxide layer on silicon substrates using a hydrofluoric acid treatment, Ag atoms bind strongly to the energetically favorable silicon atoms leading to smooth Ag films. We compare the results for Ag deposited on HF treated and untreated Si substrates for different Ag thicknesses. Our results show that HF acid treatment and annealing lead to a significant reduction in the surface roughness (~0.5 nm), narrower peak-to-valley height distribution, and higher Kurtosis. Continuous Ag films were obtained down to Ag thickness of 5 nm. We expect our results to play a crucial role in minimizing electronic and optical losses for optoelectronic, plasmonic and optical metamaterial devices.

1. Introduction

The use of metallic films with thicknesses of a few to a few tens of nanometers is central to many research fields and technologies. Ultrathin noble metallic films, e.g., silver (Ag), gold (Au), and aluminum (Al) are used as building blocks for plasmonic devices, metamaterials [1] and metasurfaces [2], and nanoelectronic devices [3]. This is due to their high electrical conductivity and low optical losses, mainly in the visible-NIR wavelength range. The applications and devices that rely on ultrathin noble metallic films are versatile and numerous, including bio-sensing [4], Water Sanitation/desalination [5], enhanced spontaneous emission rate [6, 7], and enhanced photoelectric emission [8].

However, thin metallic films deposited on oxides tend to exhibit a Vollmer-Weber (VW) growth mode, i.e., the metallic atoms tend to de-wet the surface and form islands [9]. This phenomenon leads to an increase in the surface roughness of the deposited films, which degrades the efficiency of thin-film devices. In addition, depositing a continuous ultrathin film (thickness <10 nm) is challenging, i.e., there exists a percolation thickness below which the deposited film is not continuous. High surface roughness and lack of continuity increase the resistivity of the deposited film, increase the optical losses of the film, and decrease the surface plasmon polariton propagation length, i.e., degrades its electronic and optical properties [3, 10].

In particular, minimizing the optical losses in plasmonic devices has been the center of extensive research which has been realized by adding gain material to the plasmonic system to compensate for plasmonic losses [11], operating at long (IR) wavelengths where optical losses are low, minimizing the field confinement inside

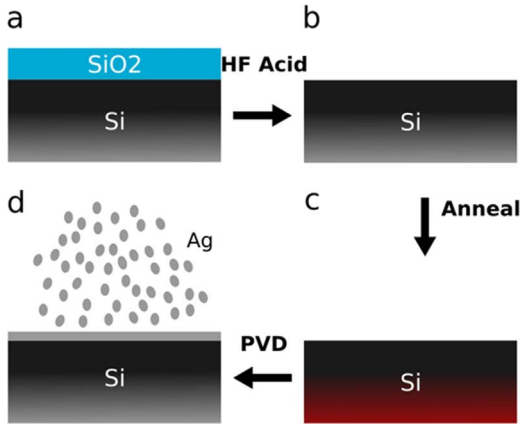

Figure 1. Fabrication of smooth Ag films: (a) Silicon substrates have a native or grown Silicon oxide layer. (b) We remove the native oxide on Si substrates using HF acid treatment. (**c**) Annealing the Si substrate evaporates metal complexes remaining on the Si substrate. (d) Depositing Ag atoms via physical vapor deposition on a bare Si substrate increases its wettability and lead to smooth Ag films.

the metal [2], or by creating smoother plasmonic films to decrease electron-defect scattering [10]. Realization of smooth plasmonic films deposited via physical vapor deposition was demonstrated using various methods, e.g., deposition on special substrates [12], optimizing the deposition process [13] and using a seed wetting layer.

To obtain a smooth film, the surface adhesive force must be higher than the adatom cohesive force leading to a Frank-van der Merwe (FM) growth mode [9]. To do so, previous works showed that depositing Germanium (Ge) [3, 14] or a copper (Cu) [15] wetting layers significantly decreases the surface root mean square roughness (R_{rms}) of Ag films down to ~0.7 nm and 0.5 nm, respectively [3, 14, 15]. This is because the bond dissociation energy between Ag atoms ($H_{Ag-Ag} = 162$ KJ mol^{-1}) is lower than that of Ag and Ge and Ag and Cu atoms which are $H_{Ag-Ge} = 174.5$ KJ mol^{-1} and $H_{Ag-Cu} = 171.5$ KJ mol^{-1}, respectively [16]. The Ag–Ag bond causes deposited Ag atoms to cluster. Consequently, creating a stronger bond between Ag atoms and a seed layer of Ge or Cu results in smoother films. Interestingly, the Ag–Si bond disassociation energy is $H_{Ag-Si} = 185.1$ KJ mol^{-1} [16]. This suggests that in leu of depositing a seed layer on an SiO_2/Si substrate [3], a possible alternative is to directly deposit Ag on Si by removing the SiO_2 layer. We note here that smooth thin film can be directly obtained using atomic layer deposition [17] and DC magnetron sputtering [18].

In this work, we create smooth Ag films deposited via thermal physical vapor deposition by removing the SiO_2 layer from Si surface with hydrofluoric (HF) acid. We show that removing the SiO_2 layer prior to depositing the Ag film and annealing the Ag film substantially increase the surface smoothness with surface roughness ~0.5 nm. Continuous Ag films down to 5 nm in thickness are obtained. The deposited Ag films enjoy significantly lower root-mean-square surface roughness, narrower grain-size distribution, and higher Kurtosis.

2. Experimental section

As purchased p doped Si substrates have a native or grown oxide layer (figure 1(a)). Removing the native oxide layer of Si using HF acid treatment (figure 1(b)) was demonstrated previously. We added 5 ml of HF with a concentration $\geqslant$40% to 110 ml DI water. The Si samples were dipped inside the solution for 2 min. After washing with the DI water, the samples were dried with N_2 and placed inside the glove box to avoid re-oxidation of the Si. Ag silver pellets (99.999% purity from Sigma-Aldrich) are then deposited via thermal vapor deposition. Thermal evaporator (Beijing Technol Co., Ltd) was used to deposit the thin film. Ag thin films of 5 nm, 10 nm and 20 nm thickness were deposited via thermal vapor deposition method on Si substrate. The film thickness was determined using a calibrated quartz crystal monitor.

Three types of Si substrates were studied; untreated Si substrates, Si substrate treated with HF acid (HF/Si), and HF treated Si substrate annealed at 150 °C for 3 min on a hot plate (annealed/HF/Si). Vacuum annealing of the HF treated Si substrate assists in volatilizing any metal complexes remaining on the Si substrate [19]. These metal complexes can act as nucleation sites that may limit the formation of homogenous and smooth Ag films. We note that annealing the treated Si substrate increases the surface roughness of the HF treated Si substrate prior to Ag deposition. Minimum surface roughness was observed at annealing temperature of 150 °C which was used in all the samples. The thin films were deposited at 3×10^{-7} torr pressure and at 100-Watt and the deposition rate was maintained at 6 Å s^{-1}. We also note that we annealed the Si substrate prior to Ag film deposition which differs from the rapid post deposition annealing process demonstrated previously [14].

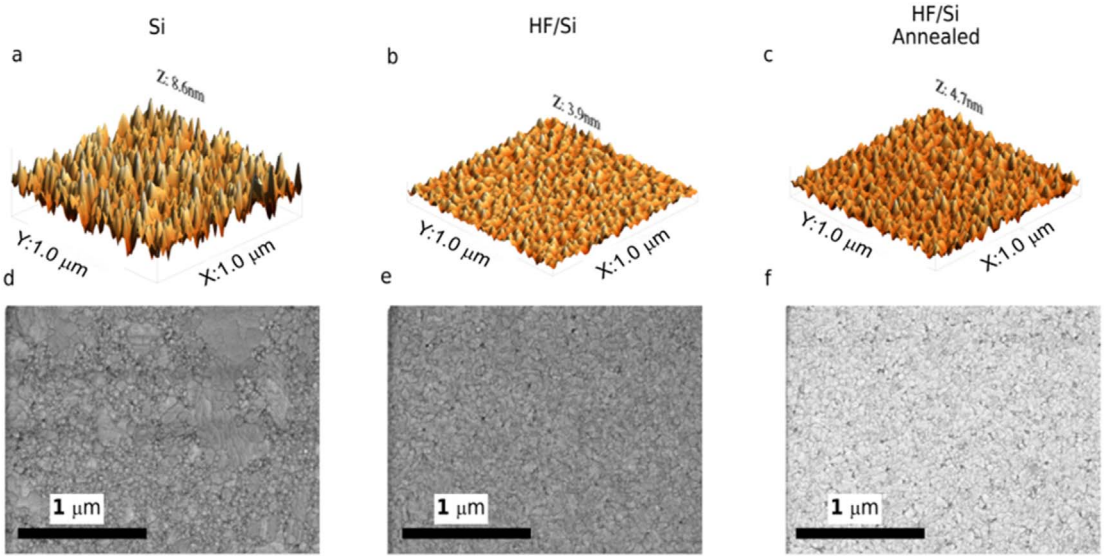

Figure 2. Surface characterization of 20 nm Ag film. (a)–(c) AFM images of a 20 nm Ag film deposited on (a) untreated Si substrate, (b) HF/Si substrate, and (c) annealed/HF/Si substrate. A significant decrease in surface roughness is clear following HF treatment. (d)–(f) SEM images of a 20 nm Ag film deposited on (d) untreated Si substrate, (e) HF/Si substrate, and (f) annealed/HF/Si substrate.

The surface roughness of the prepared samples was measured using Bruker Multimode-8 Atomic force microscope and surface morphology was studied by using FE-Scanning electron microscope HITACHI, S-4800. The root mean square roughness (R_{rms}) is the square root of the all the surface heights and is sensitive to large deviations from the mean height.

Kurtosis is a dimensionless measure of the combined weight of a distribution's tails relative to the center of the distribution. We use it here to characterize the height distribution. The Kurtosis 'κ' is given by

$$\kappa = \frac{1}{{R_{rms}}^4} \frac{1}{N} \sum_{j=1}^{N} Z_j^4$$

where N is the sum of all counts, and Z is the measured height.

3. Results and discussion

Figures 2(a)–(c) show atomic force microscopy (AFM) surface topography images over a 1 μm $\times$ 1 μm area of a 20 nm Ag film deposited on an Si, HF/Si and annealed/HF/Si substrates, respectively. Clearly, after HF treatment the surface roughness dramatically decreases. The measured R_{rms} is 1.63 nm, 1.13 nm, and 0.72 nm for Si, HF/Si and annealed/HF/Si substrates, respectively. Figures 2(d)–(f) show the scanning electron microscope (SEM) images of the Si, HF/Si and annealed/HF/Si substrates, respectively. For the untreated Si sample (figure 2(c)), the Ag film consists of metallic islands with large distribution of grains, irregular shapes, and multiple cracks and voids, i.e., symptoms of the VW growth mode. On the other hand, Ag deposited on HF/Si and annealed/HF/Si substrates show uniform Ag film growth with similar grain size distribution and limited voids and cracks, i.e., the film growth mode is no longer a VW growth mode.

To test the efficacy of our approach for ultrathin Ag films we deposited 5 nm thick Ag films on the three substrates. Figures 3(a)–(c) show atomic force microscopy (AFM) surface topography images over a 1 μm $\times$ 1 μm area of a 5 nm Ag film deposited on an Si, HF/Si and annealed/HF/Si substrates, respectively, which also shows a noticeable decrease in the surface roughness after HF treatment. The measured surface R_{rms} is 1.2 nm, 0.85 nm, and 0.95 nm for Si, HF/Si and annealed/HF/Si substrates, respectively. We note that the R_{rms} of the film deposited on the annealed/HF/Si substrate slightly increased compared to the film on HF/Si substrate. As we mentioned earlier annealing is commonly utilized to evaporate metal complexes remaining on the Si substrate [19]. On the other hand, annealing increases the R_{rms} of the as treated Si substrate. Consequently, for thicker films the evaporation of the metal complexes facilitates the Ag adatom adhesion to the Si substrate leading to smoother Ag films. However, for thinner Ag films, e.g., with 5 nm thickness, the overall R_{rms} can may be strongly affected by the substrate's initial roughness. The advantage of annealing is evident, however, when considering other surface parameters, e.g., peak-to-valley size distribution and Kurtosis, as we will detail later. Figures 3(d)–(f) show the scanning electron microscope (SEM) images of the Si, HF/Si and annealed/HF/Si

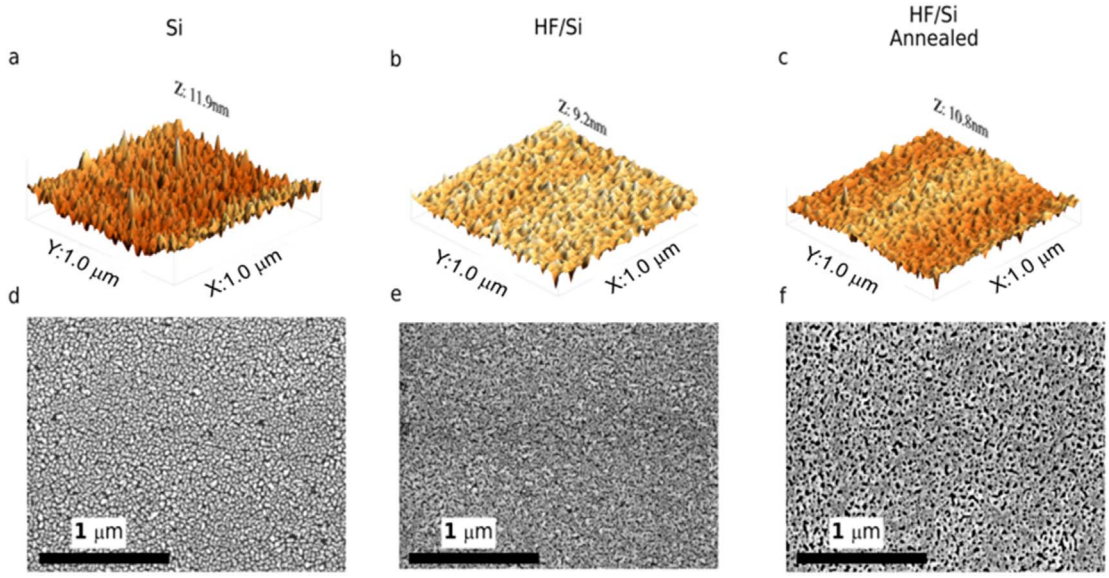

Figure 3. Surface characterization of 5 nm Ag film. (a)–(c) AFM images of a 5 nm Ag film deposited on (a) untreated Si substrate, (b) HF/Si substrate, and (c) annealed/HF/Si substrate. A significant decrease in surface roughness is clear following HF treatment. (d)–(f) SEM images of a 5 nm Ag film deposited on (d) untreated Si substrate, (e) HF/Si substrate, and (f) annealed/HF/Si substrate. The SEM images show that prior to HF treatment the Ag film is below its percolation thickness. After HF treatment and annealing, a continuous Ag film with voids is obtained.

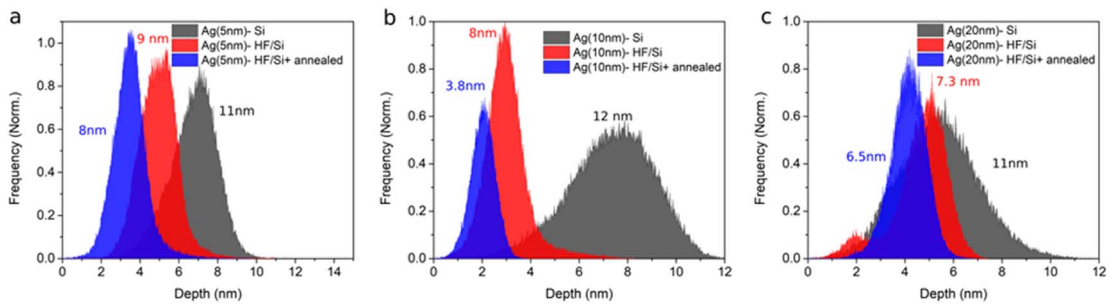

Figure 4. Histograms of the 2D surface-height values obtained from AFM image analysis for an Ag film with thickness (a) 5 nm, (b) 10 nm, and (c) 20 nm. The histograms are obtained for Ag films deposited on untreated Si substrates (black), HF/Si substrates (red) and annealed/HF/Si substrates (blue). The results show that the narrowest peak-to-valley height values (annotated in the figures) are obtained for Ag films deposited on annealed/HF/Si substrates.

substrates, respectively. For the untreated Si sample (figure 3(c)), the Ag film consists of nanoparticles, i.e., the 5 nm Ag film is below the percolation thickness. Consequently, a 5 nm Ag film is not continuous and suffers from low electronic and optical quality as observed in previous reports [3, 15]. Following HF treatment, we see interconnected grains which can allow for a decent electron transport (figure 3(e)). Depositing the 5 nm film on the annealed/HF/Si substrate leads to a continuous film with voids (figure 3(f)). These results show that our approach enables the creation of continuous, ultrathin plasmonic films.

Histograms of the 2D surface height values obtained from AFM measurements are shown in figures 4(a)–(c) for an Ag layer with 5 nm, 10 nm, and 20 nm thickness, respectively. The results compare the surface roughness of the Ag films deposited on untreated Si (black), HF/Si (red), and annealed/HF/Si (blue). For all Ag thicknesses, the peak-to-valley size distribution of the untreated Si sample is largest indicating a major variation in the sizes of grain and existence of voids and cracks. On the other hand, removing the oxide layer provides narrower peak-to-valley values which is further reduced after annealing. For instance, the peak-to-valley height R_{PV} of a 10 nm Ag film reduced from ~12 nm for an untreated Si substrate to ~3.8 nm for annealed HF/Si substrate (figure 4(b)). Although R_{rms} of the 5 nm Ag film deposited on the annealed/HF/Si substrate was relatively higher than that deposited on HF/Si substrate, we can clearly see a reduction in its R_{PV} which is an important measure of the surface roughness (figure 4(a)).

Table 1 summarizes the main results of all the samples in terms of R_{rms}, peak-to-valley distribution R_{PV}, and Kurtosis. The surface roughness of a 10 nm Ag film is 1.73 nm (Si), 0.87 nm (HF/Si), and 0.48 nm (annealed/

Table 1. Summary of surface morphology parameters for 5 nm, 10 nm, and 20 nm Ag films deposited on Si, HF/Si, and annealed/HF/Si substrates.

	Peak-to-valley roughness- R_{PV} (nm)	RMS roughness- R_{rms} (nm)	Kurtosis κ
5 nm Ag- Si	11	1.2	0.4213
5 nm Ag- HF/Si	9	0.85	1.922
5 nm Ag- annealed HF/Si	8	0.95	0.9159
10 nm Ag- Si	12	1.73	0.05
10 nm Ag- HF/Si	8	0.87	3.27
10 nm Ag- annealed HF/Si	3.8	0.49	2.95
20 nm Ag- Si	11	1.63	0.0005
20 nm Ag- HF/Si	7.3	1.13	0.946
20 nm Ag- annealed HF/Si	6.5	0.72	0.32
Si	8.5	1.49	12.9
HF/Si	2.7	0.39	1.005
Annealed HF/Si	2.6	1.6	2.15

HF/Si) which is lower than what was reported previously using Ge seed layer [3] and comparable to the R_{rms} of Cu seed layer [15]. We note that using an Si seed layer differs from using an Si substrate. Formica *et al* [15] used an Si seed layer which lead to a rougher Ag film compared to a Cu seed layer. Their results indicated that the Si atoms acted as a nucleation dot for the growth of Ag islands. On the other hand, the growth of Ag films on an Si substrate provides homogenous nucleation sites that creates smoother surfaces. Table 1 also show the Kurtosis results for all the samples. Higher Kurtosis can indicate a sharper peak which reflects the homogeneity of the grain height across the film. From table 1 and figures 4(a)–(c), we can see that annealed/HF/Si samples have considerably higher Kurtosis and sharper peaks compared to untreated Si substrates. This reflects the predominance of a single grain height for the treated samples compared to untreated samples. We note that HF/Si samples have the highest Kurtosis even when compared to annealed/HF/Si samples. This is likely due to the increase in the surface roughness of the annealed/HF/Si substrates due to annealing which can increase the relative value of the distribution's tail relative to its peak. The surface morphology parameters for the Si, HF/Si and annealed HF/Si substrate shows that there is no direct correlation between the substrate's morphology and the morphology of the deposited films. Finally, although HF treatment of Si can lead to the formation of Si–F and Si–H bonds, it is unlikely that this would deteriorate the Ag adhesion to the substrate since the bond dissociation energy of the Ag–F and Ag–H bonds is $H_{Ag-F} = 357\ KJ/mol^{-1}$ and $H_{Ag-H} = 202\ KJ/mol^{-1}$, respectively, which is higher than that of the Ag–Ag bond $H_{Ag-Ag} = 162\ KJ/mol^{-1}$ [16].

4. Conclusion

We showed that by removing the oxide layer existing on an Si substrate via HF acid treatment, we can significantly improve the smoothness of deposited Ag films in terms of decreasing the surface rms roughness, narrowing the peak-to-valley roughness distribution, and increasing the distribution Kurtosis. Our method compliments other existing methods to increase the quality of plasmonic and metallic films deposited on Silicon substrates. Indeed, we provide a more economic method as we do not require using any seed layer. Moreover, our method is CMOS compatible and avoid introducing additional materials, e.g., Ge, which may degrade the optical properties of the deposited film. While we do not expect this method to be used for multilayer structures as in the case of using Ge seed layer [14], we expect that it can at least decrease the overall roughness of the multilayer structure without jeopardizing its optical properties. From a practical standpoint, we recommend the annealing and HF treatment in general. However, for applications where minimizing the surface roughness is crucial, avoiding the annealing process for 5 nm films is recommended. Using other acids that remove the oxide layer is also possible. Our method can certainly be extended to other plasmonic metals. For instance, we expect that our method would increase the smoothness of gold (Au) films. The bond dissociation energy of Au-Au atoms is $H_{Au-Au} = 226.2\ KJ/mol^{-1}$ while for Au–Si atoms it is $H_{Au-Si} = 304.6\ KJ/mol^{-1}$ [16].

Acknowledgments

The authors would like to acknowledge the funding from the National Natural Science Foundation of China (NSFC) (91750205, 11804334), Bill & Melinda Gates Foundation (INV-009181), Jilin Provincial Science & Technology Development Project (20180414019GH), K.C. Wong Education Foundation (GJTD-2018-08).

ORCID iDs

Muhammad Asad https://orcid.org/0000-0001-5095-939X
Mohamed ElKabbash https://orcid.org/0000-0003-3795-7714

References

[1] Cortes C L, Newman W, Molesky S and Jacob Z 2012 Quantum nanophotonics using hyperbolic metamaterials *J. Opt.* **14** 063001
[2] Zhang J, ElKabbash M, Wei R, Singh S C, Lam B and Guo C 2019 Plasmonic metasurfaces with 42.3% transmission efficiency in the visible *Light: Science & Applications* **8** 53
[3] Logeeswaran V, Kobayashi N P, Islam M S, Wu W, Chaturvedi P, Fang N X, Wang S Y and Williams R S 2009 Ultrasmooth silver thin films deposited with a germanium nucleation layer *Nano Lett.* **9** 178–82
[4] Sreekanth K V *et al* 2019 Phase-change-material-based low-loss visible-frequency hyperbolic metamaterials for ultrasensitive label-free biosensing *Adv. Opt. Mater.* **7** 1900081
[5] Singh S, ElKabbash M, Li Z, Li X, Regmi B, Madsen M, Jalil S. A., Zhan Z, Zhang J and Guo C 2020 Solar-trackable super-wicking black metal panel for photothermal water sanitation *Nature Sustainability* 57
[6] Chamoli S K, ElKabbash M, Zhang J and Guo C 2020 Dynamic control of spontaneous emission rate using tunable hyperbolic metamaterials *Opt. Lett.* **45** 1671–4
[7] ElKabbash M, Miele E, Fumani A K, Wolf M S, Bozzola A, Haber E, Shahbazyan T V, Berezovsky J, De Angelis F and Strangi G 2019 Cooperative energy transfer controls the spontaneous emission rate beyond field enhancement limits *Phys. Rev. Lett.* **122** 203901
[8] Hwang TY, Vorobyev AY and Guo C 2009 Surface-plasmon-enhanced photoelectron emission from nanostructure-covered periodic grooves on metals *Physical Review B* **79** 085425
[9] Oura K, Lifshits V, Saranin A, Zotov A and Katayama M 2013 *Surface Science: an Introduction* (Berlin: Springer)
[10] Khurgin J B 2015 How to deal with the loss in plasmonics and metamaterials *Nat. Nanotechnol.* **10** 2–6
[11] ElKabbash M, Sousa-Castillo A, Nguyen Q, Mariño-Fernández R, Hoffman N, Correa-Duarte M A and Strangi G 2017 Tunable black gold: controlling the near-field coupling of immobilized Au nanoparticles embedded in mesoporous silica capsules *Adv. Opt. Mater.* **5** 1700617
[12] Malureanu R and Lavrinenko A 2015 Ultra-thin films for plasmonics: a technology overview *Nanotechnology Reviews* **4** 259–75
[13] McPeak K M, Jayanti S V, Kress S J P, Meyer S, Iotti S, Rossinelli A and Norris D J 2015 Plasmonic films can easily be better: rules and recipes *ACS Photonics* **2** 326–33
[14] Chen W, Thoreson M D, Ishii S, Kildishev A V and Shalaev V M 2010 Ultra-thin ultra-smooth and low-loss silver films on a germanium wetting layer *Opt. Express* **18** 5124–34
[15] Formica N, Ghosh D S, Carrilero A, Chen T L, Simpson R E and Pruneri V 2013 Ultrastable and atomically smooth ultrathin silver films grown on a copper seed layer *ACS Applied Materials & Interfaces* **5** 3048–53
[16] Luo Y-R and Kerr J 2012 Bond dissociation energies *CRC Handbook of Chemistry and Physics* **89** 89
[17] Im H, Wittenberg N J, Lindquist N C and Oh S-H 2012 Atomic layer deposition (ALD): a versatile technique for plasmonics and nanobiotechnology *J. Mater. Res.* **27** 663
[18] Sun X, Hong R, Hou H, Fan Z and Shao J 2007 Thickness dependence of structure and optical properties of silver films deposited by magnetron sputtering *Thin Solid Films* **515** 6962–6
[19] Rużyłło J 1998 *Proc. of the Fifth Int. Symp. on Cleaning Technology in Semiconductor Device Manufacturing* (The Electrochemical Society)